Weakening of the Atlantic Niño variability under global warming

Lander Crespo (lander.crespo@uib.no)
University of Bergen and Bjerknes Centre for Climate Research https://orcid.org/0000-0003-1273-4303

Physical Sciences - Article

Keywords:

Posted Date: January 4th, 2022

DOI: https://doi.org/10.21203/rs.3.rs-829552/v1

Version of Record: A version of this preprint was published at Nature Climate Change on September 1st, 2022. See the published version at https://doi.org/10.1038/s41558-022-01453-y.

Weakening of the Atlantic Niño variability under global warming

Lander R. Crespo[1,2] , Arthur Prigent[3], Noel Keenlyside[1,2], Shunya Koseki[1,2], Lea Svendsen[1,2], Ingo Richter[4], Emilia Sánchez-Gómez[5]

[1] Geophysical Institute, University of Bergen, Norway
[2] Bjerknes Center for Climate Research, University of Bergen, Norway
[3] GEOMAR, Kiel, Germany
[4] Japan Agency for Marine-Earth Science and Technology, JAMSTEC, Japan
[5] CERFACS, Toulouse, France

The Atlantic Niño is one of the most important tropical patterns of interannual climate variability, with major regional and global impacts. How global warming will influence the Atlantic Niño has been hardly explored, because of large climate model errors. We show for the first time that the state-of-the-art climate models robustly predict that equatorial Atlantic Niño variability will weaken in response to global warming. This is primarily because subsurface and surface temperature variations decouple as the upper equatorial Atlantic Ocean warms. The weakening is predicted by most (>80%) models following the highest emission scenarios in the Coupled Model Intercomparison Project Phases 5 and 6 considered here. These indicate a reduction in variability by the end of the century of 12-17%, and as much as 25% when accounting for model errors. Weaker Atlantic Niño variability will have major consequences for global climate and the skill of seasonal predictions.

The Atlantic Niño phenomenon exhibits many similarities to the stronger El Niño/Southern Oscillation[1,2] (ENSO) in the Pacific. The eastern equatorial Atlantic is anomalously warm, surface trade winds relax and rainfall shifts equatorward during positive Atlantic Niño[3-5] events. The sea surface temperature (SST) anomalies in the equatorial cold tongue can reach 1.5ºC and thermocline (20ºC isotherm) depth anomalies can exceed 30 m in boreal summer when the events peak. Opposite conditions are found during negative events. Coupled ocean-atmosphere interactions—Bjerknes positive and delayed negative feedbacks—similar to those in the Pacific can explain most Atlantic Nino variability, but other mechanisms can contribute substantially to equatorial SST anomalies[6]. The Atlantic Niño has

significant impacts on the climate[7-9] and marine biogeochemistry[10,11] in the tropical Atlantic sector, on ENSO[12-16], and extra-tropical climate[17-20].

Recent studies have shown a weakening of the Atlantic Niño variability in the last decades[21-23]. The changes in eastern equatorial Atlantic SST variability have been attributed to the combined effect of a weakening of the Bjerknes feedback[24] (BF) and increased heat flux damping[22,23], and to a basin-wide warming related to climate change[24]. These studies used observational and reanalysis datasets to investigate changes in the SST variability during the historical period.

Extensive analysis of the projections from the Coupled Model Intercomparison Project (CMIP) indicate that ENSO events will become stronger under global warming, but large uncertainties exist[25-29]. Large climate model biases in the tropical Atlantic sector[30-33] have discouraged the climate community from carrying out similar in-depth assessment of climate change in the area. However, we will show that such biases do not preclude a more robust assessment of global warming impacts on Atlantic Niño variability than has been achieved in the Pacific.

Weakened variability of the equatorial Atlantic SST

To investigate how the SST variability in the eastern equatorial Atlantic will change under global warming, we use historical simulations and the future highest emission scenario simulations from the CMIP5[34] and CMIP6[35] archive. The comparison between the historical (1950-99) and future scenario (2050-99) periods in the CMIP models shows that the SST variability in the eastern equatorial Atlantic sector in June-July-August (JJA) is reduced in the majority of the CMIP models (33 out of 40) (Fig. 1a and Table 1). The multi-model ensemble mean of CMIP5 (CMIP6) shows a reduction of the SST variability of 12% (17%) in the future scenario simulation with respect to the historical simulation (Table 1). The surface zonal winds in the western Atlantic sector also show a reduced future variability in May-June-July (MJJ) season in the CMIP5 and CMIP6 models with only 3 out of 40 models presenting an increased variability (Fig. 1d, Table 1). The ensemble mean of the standard deviation of the MJJ zonal wind anomalies (UAS hereafter) is reduced by 13% in CMIP5 and by 17% in CMIP6, which corresponds very well to the amplitude of the reduction in JJA SST variability (Table 1). The reduction of the zonal surface winds in the western equatorial Atlantic is consistent with a more stratified atmosphere in a future warmer climate[36].

Table 1. List of CMIP5 and CMIP6 models used in this study (first column). Standard deviation of the JJA ATL3-averaged SST anomalies and the MJJ ATL4-averaged UAS anomalies (second column) in brackets, during 1950-1999 and 2050-2099. The reduction is relative to the 1950-1999 period. ENS is the multi-model ensemble mean of the CMIP5 and CMIP6. JJA ATL3-averaged SST change (fourth column), defined as the difference of the 2050-2099 mean minus the 1950-1999 mean.

No.	Models	ATL3 JJA SST Variability [°C] (ATL4 MJJ UAS variability [m.s^{-1}]) 1950-1999	2050-2099	Reduction [%]	ATL3 JJA SST Change [K]
0	ACCESS-CM2	0.54 (1.41)	0.38 (1.08)	30 (23)	3.52
1	ACCESS-ESM1-5	0.68 (1.21)	0.53 (0.87)	22 (28)	3.14
2	BCC-CSM2-MR	0.31 (0.61)	0.28 (0.55)	10 (10)	2.18
3	CAMS-CSM1-0	0.39 (0.98)	0.28 (0.68)	28 (31)	0.8
4	CanESM5	0.54 (0.77)	0.34 (0.43)	37 (44)	3.96
5	EC-Earth3	0.63 (1.12)	0.69 (1.16)	-10 (-4)	2.49
6	EC-Earth3-Veg	0.65 (1.05)	0.60 (1.09)	8 (-4)	2.50
7	GFDL-ESM4	0.54 (0.85)	0.52 (0.76)	4 (11)	2.27
8	INM-CM4-8	0.34 (0.57)	0.26 (0.49)	24 (14)	2.23
9	INM-CM5-0	0.36 (0.60)	0.27 (0.52)	25 (13)	2.04
10	IPSL-CM6A-LR	0.68 (0.88)	0.52 (0.77)	24 (12)	3.56
11	MIROC6	0.51 (0.97)	0.32 (0.87)	37 (10)	2.77
12	MPI-ESM1-2-HR	0.56 (0.88)	0.35 (0.60)	38 (32)	1.81
13	MPI-ESM1-2-LR	0.32 (1.00)	0.35 (0.81)	-9 (19)	1.68
14	MRI-ESM2-0	0.7 (1.18)	0.59 (1.02)	16 (14)	3.36
15	NESM3	0.37 (0.81)	0.39 (0.61)	-5 (21)	2.34
	ENS	**0.51 ±0.14 (0.93 ±0.23)**	**0.42 ±0.13 (0.77 ±0.22)**	**17 ±13 (17 ±12)**	**2.70±0.58**
16	ACCESS1-0	0.41 (0.72)	0.29 (0.68)	29 (6)	3.07
17	ACCESS1-3	0.52 (0.89)	0.50 (0.80)	4 (10)	3.16
18	CMCC-CESM	0.46 (1.26)	0.69 (1.35)	-50 (-7)	2.51
19	CMCC-CMS	0.38 (0.85)	0.37 (0.82)	3 (4)	3.02
20	CMCC-CM	0.37 (0.74)	0.35 (0.69)	5 (7)	2.75
21	CNRM-CM5	0.23 (0.88)	0.22 (0.84)	5 (5)	2.11
22	CSIRO-Mk3-6-0	0.46 (0.56)	0.33 (0.34)	28 (39)	2.59
23	GFDL-CM3	0.81 (1.11)	0.69 (0.96)	15 (14)	2.99
24	GFDL-ESM2M	0.90 (1.60)	0.97 (1.50)	-8 (6)	2.36
25	GISS-E2-H-CC	0.31 (0.86)	0.28 (0.63)	10 (26)	1.91
26	GISS-E2-H	0.35 (0.65)	0.27 (0.59)	23 (9	2.16
27	GISS-E2-R-CC	0.22 (0.55)	0.19 (0.46)	14 (16)	1.98
28	GISS-E2-R	0.24 (0.57)	0.19 (0.52)	21 (9)	1.91
29	HadGEM2-CC	0.82 (1.18)	0.60 (1.01)	27 (14)	3.41
30	IPSL-CM5A-LR	0.48 (0.55)	0.45 (0.52)	6 (5)	3.83
31	IPSL-CM5A-MR	0.44 (0.57)	0.38 (0.48)	14 (16)	3.70
32	IPSL-CM5B-LR	0.31 (1.31)	0.32 (1.03)	-3 (21)	2.08
33	MIROC-ESM-CHEM	0.33 (0.42)	0.26 (0.35)	21 (17)	3.27
34	MIROC-ESM	0.37 (0.42)	0.27 (0.35)	27 (17)	3.25
35	MIROC5	0.63 (1.31)	0.41 (0.82)	35 (37)	3.10
36	MPI-ESM-LR	0.43 (0.86)	0.34 (0.64)	21 (26)	2.80
37	MPI-ESM-MR	0.48 (0.77)	0.36 (0.69)	25 (10)	2.76
38	MRI-CGCM3	0.52 (0.98)	0.4 (0.95)	23 (3)	2.43
39	NorESM1-M	0.43 (1.13)	0.49 (0.99)	-14 (12)	1.77
	ENS	**0.45 ±0.18 (0.86 ±0.31)**	**0.40 ±0.18 (0.75 ±0.29)**	**12 ±18 (13 ±10)**	**2.54 ±0.79**

The reduction of the standard deviation in both SST and UAS is more pronounced and localized in the ensemble mean of CMIP6 (Fig. 1c and f) than in CMIP5 (Fig 1b and e). The weakening of the standard deviation of the MJJ zonal winds in the western equatorial Atlantic is followed by a weakening of the eastern equatorial Atlantic JJA SST variability in both CMIP5 (Fig. 1b and e) and CMIP6 (Fig. 1c and f) ensemble means, suggesting that the reduced wind variability may be the cause of

the reduced SST variability. However, the linear regression between the two variables explains only 32% of the variance (Fig. S1). Consequently, there are other mechanisms that play an important role in the reduction of the standard deviation of the SST in the eastern equatorial Atlantic.

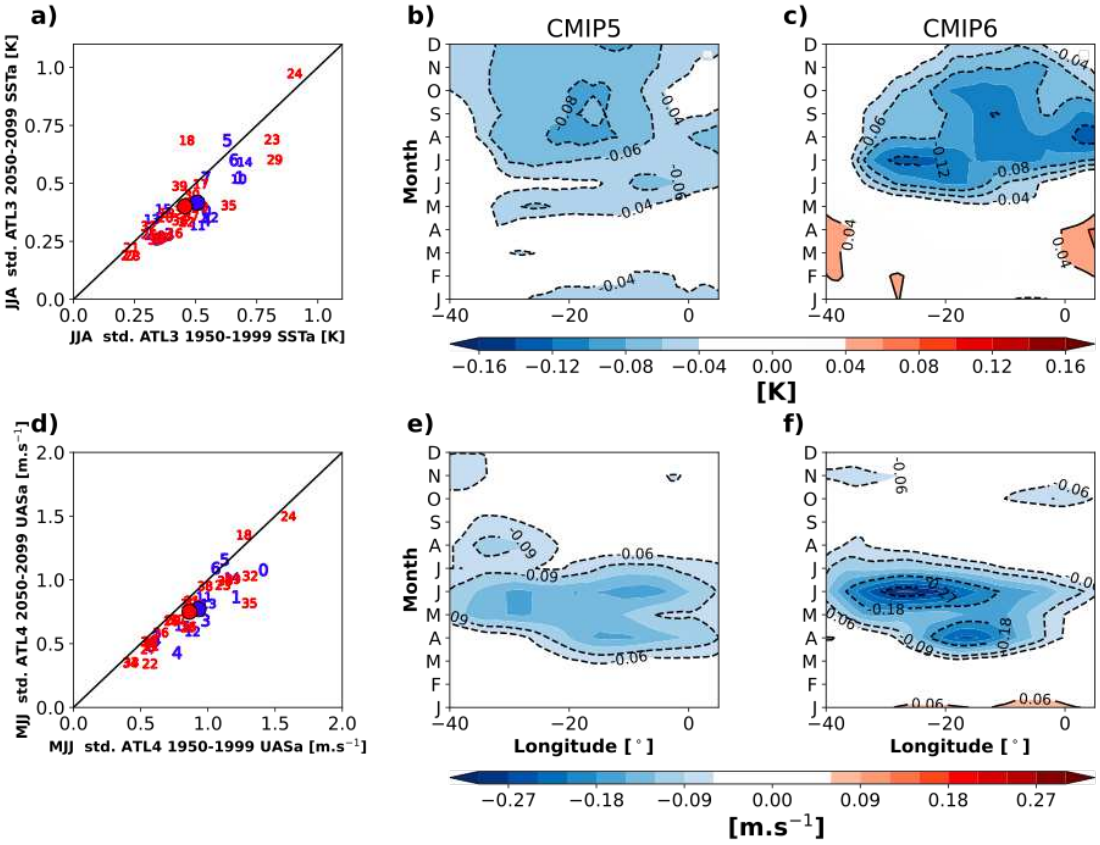

Figure 1. Weakening of the eastern equatorial Atlantic SST variability. (a) Scatter plot of the JJA average standard deviation of the SSTa for the historical period (1950-99) in the x axis against the standard deviation of SSTa for the scenario period (2050-99) in the y axis. The black line represents the no-change line and is added for easier interpretation. Difference between the means of the 2050-2099 and the 1950-1999 periods standard deviation of the SST anomalies for the ensemble mean of CMIP5 (b) and CMIP6 (c) models, along the equator and averaged between 3˚S and 3˚N. Same as (b) and (c) for the surface zonal wind anomalies of the CMIP5 (e) and CMIP6 (f) models, along the equator and averaged between 3˚S and 3˚N. (d) Scatter plot of the MJJ average standard deviation of the UASa for the historical period (1950-99) in the x axis against the standard deviation of UASa for the scenario period (2050-99) in the y axis. The black line represents the no-change line and is added for easier interpretation. The blue (red) numbers correspond to the CMIP6 (CMIP5) models listed in Table 1. The blue (red) circle shows the ensemble mean of CMIP6 (CMIP5) models.

Weakened ocean-atmosphere coupling

We explore the relative importance of the dynamical and thermodynamical drivers of the future changes in the SST, through the BF components and the net heat flux damping (Methods). The basin-wide weakening of the SST variability and winds in the future scenario simulation might be related to a weakening of the BF. The changes in variability in CMIP5 and CMIP6 are rather similar and therefore, we will consider all CMIP models together in this section.

Both ensemble means of CMIP5 and CMIP6 models show a small change of the first component of the BF (i.e. the linear regression of MJJ ATL4 zonal winds anomalies on the JJA ATL3 SSTa). A majority of the CMIP models agrees on a decrease of the 1st component of the BF; 29 out of 40 models (Fig. 2a). The second component of the BF, the thermocline slope response to western equatorial wind anomalies, shows a small reduction for CMIP models (Fig. 2b). The change in the second BF component shows less inter-model agreement than the first component of the BF with 26 out of 40 CMIP models showing a decrease of the second component of the BF. The third component of the BF, that accounts for the local response of SSTa to thermocline depth anomalies in the ATL3 region, shows the most consistent changes; with 31 out of 40 CMIP models showing a reduction of the third BF component. Both the CMIP5 and the CMIP6 multi-model ensemble means show a reduction in the strength of this relation in the future climate simulations (Fig. 2f).

The change of the third BF component between historical and future simulations is strongly related to the change in ATL3 JJA SST variability between the two periods, with a explained variance of 61% when considering all CMIP models (Fig. 2f). Contrastingly, the changes in components one and two of the BF explain only little variance of the change in SST variability, namely 19% and 18%, respectively. Therefore, the reduced sensitivity of SST to local changes in thermocline depth dominates the reduction of SST variability in the eastern equatorial Atlantic in the future scenario. However, the majority of the CMIP models largely underestimates the strength of this part of the feedback (Fig. 2c), a flaw already present in CMIP5 models[37] that still persists in the latest CMIP6 generation. Therefore, the CMIP models might underestimate the future reduction of SST variability.

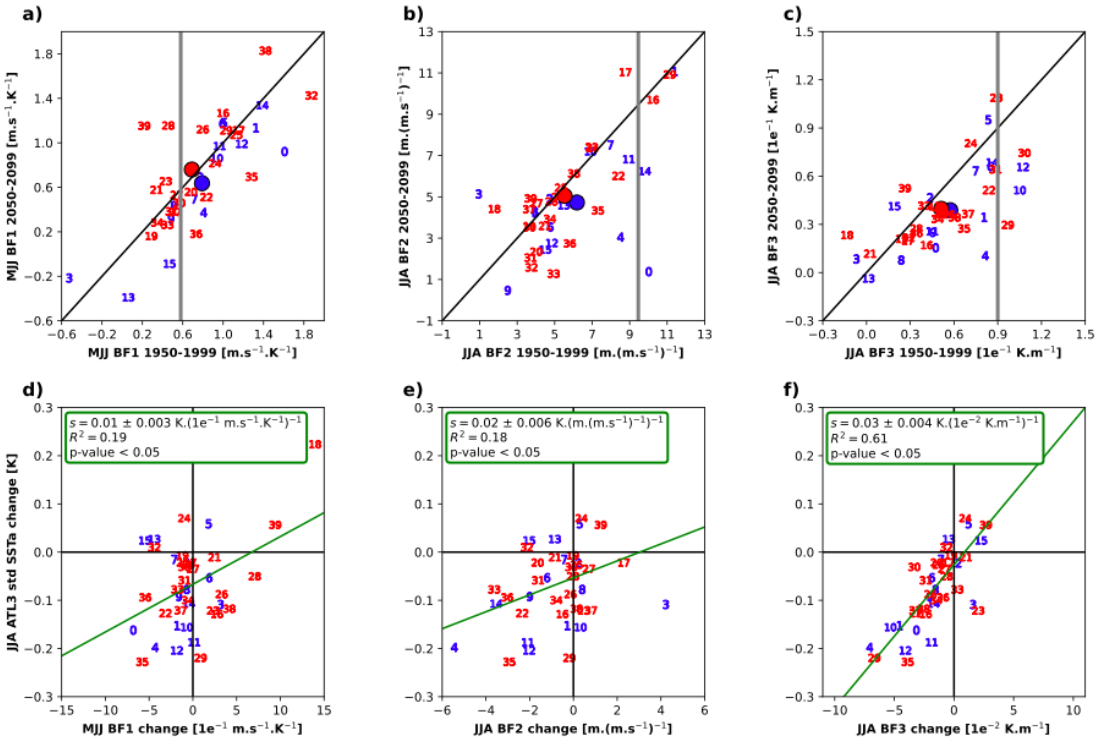

Figure 2. **Dynamical drivers of the weakening of the SST variability.** Changes between the historical and future scenario in the strength of the Bjerknes feedback (BF) components. (a) 1st component of the BF is the linear regression of ATL4 MJJ UAS anomalies against the JJA ATL3 SSTa. (b) 2nd component of the BF as the linear regression of ATL4 JJA UAS anomalies on the thermocline slope depth anomalies (aka z20 in Atl3 minus z20 in Atl4). (c) 3rd component of BF computed as the linear regression of ATL3 JJA SSTa onto the JJA ATL3 Z20 anomalies. The blue and red dots are the ensemble mean of the CMIP6 and CMIP5 ensemble, respectively. Linear regression between the change in JJA SSTa variance and the change in BF components (d, e, f). The change here is defined as the difference of the mean of the scenario period (2050-99) minus the mean of the historical period (1950-99). The vertical grey lines represent an estimation of the three components of the BF (a, b and c) from observation and reanalysis datasets.

Future mean changes of the tropical Atlantic SST

The strength of the 3rd component of Bjerknes Feedback is linked to the strength of climatological upwelling and vertical temperature stratification[38]. In particular, a weaker feedback can result from the weaker upwelling of relatively warmer subsurface waters. Despite a large intermodel spread, the SST change between historical and future scenario simulations shows a robust warming of the equatorial Atlantic cold tongue consistent with weakening of this component of the

BF (Table 1). The future scenario simulations of CMIP5 and CMIP6 models present a warming of the JJA season in the eastern equatorial Atlantic of 2.54 ± 0.79ºC and 2.70 ± 0.58ºC, respectively. The multimodel ensemble mean of the CMIP5 and CMIP6 models show a warming of 2ºC to 3ºC in the tropical Atlantic sector between the historical and the future scenario simulation (Fig. 3a,b). The spatial patterns of the future warming rate in the multimodel ensemble mean of both CMIPs are rather similar and show a strong zonally homogeneous warming along the equatorial band. The surface trade winds are projected to weaken in most of the tropical Atlantic in CMIP5, coinciding with the warming pattern. In the CMIP6 ensemble mean, the weakening of the surface trade winds is confined to the eastern equatorial Atlantic and north of 10ºN (Fig. 3a,b). Weaker equatorial trade winds will weaken equatorial upwelling, and thereby contribute to a weaker 3rd component of the BF.

The vertical section of the difference between future scenario and historical of the equatorial Atlantic ocean temperature clearly shows a stronger warming of the upper ocean, going from the surface down to about 50 meters in the eastern equatorial Atlantic, and 70 meters in the western equatorial Atlantic in the CMIP5 ensemble mean (Fig. 3c). The warming in the eastern equatorial Atlantic is even more pronounced in the CMIP6 ensemble mean (Fig. 3d). The warming of the upper levels is rather zonally homogeneous in both CMIP5 and CMIP6. However, this is not the case for the deeper levels where the eastern equatorial Atlantic is warming faster than the western side of the basin; this warming pattern could be related to changes in oceanic circulation associated with the subtropical cells and AMOC[39]. The strong warming of the upper levels in the ensemble mean of both CMIP generations leads to a deeper thermocline in the future scenario (Fig. 3c,d). As the thermocline gets deeper the coupling between the thermocline and the SST gets weaker, because the stratification at the base of the mixed layer becomes weaker. In other words, the variability in the SST is less sensitive to the variability of the thermocline, in agreement with the previously shown weakening of the third component of the Bjerknes feedback (Fig. 2c).

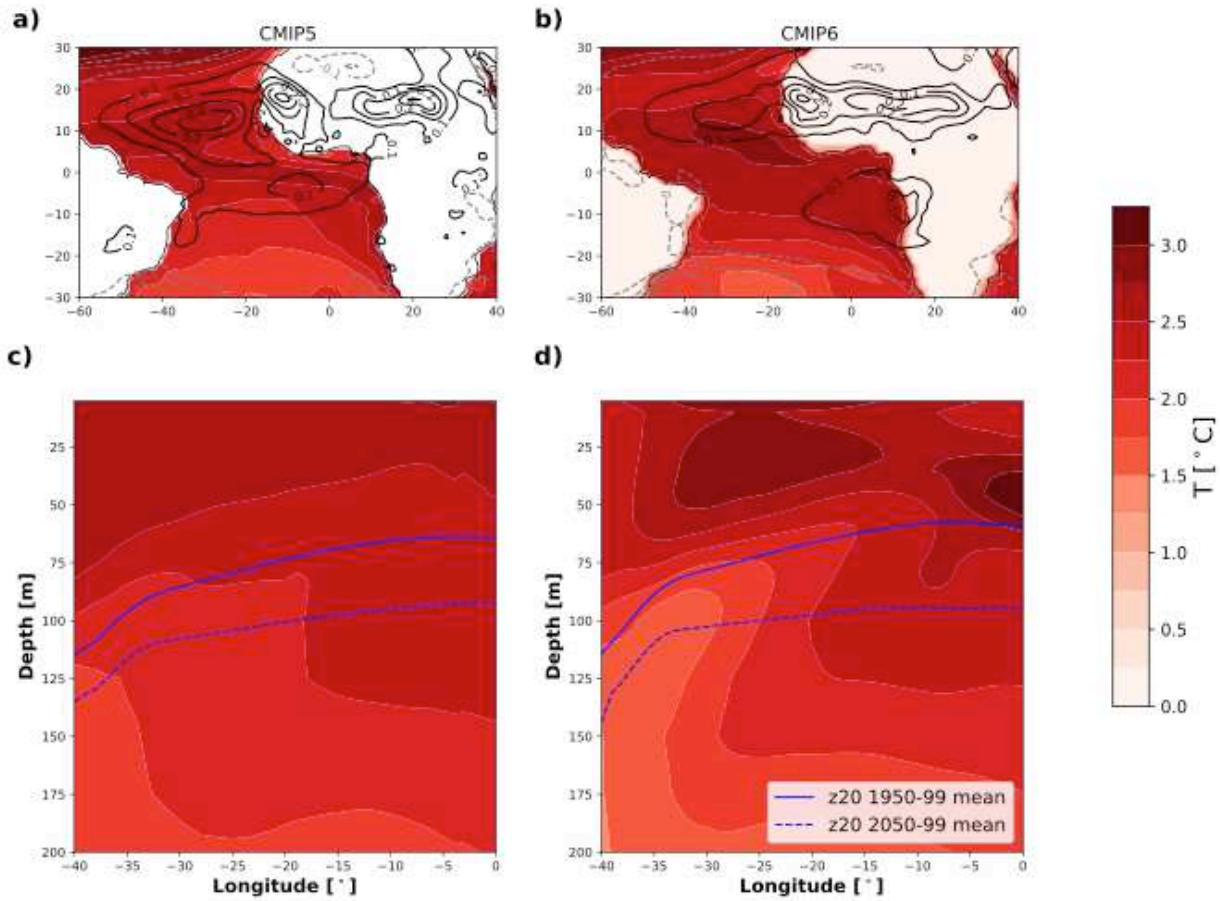

Figure 3. Mean state changes in the equatorial Atlantic. (Top row) Difference between future scenario and historical simulations of SST (in shading) and zonal surface winds (in contours) for the multi-model ensemble means of (a) CMIP5 and (b) CMIP6. The dashed (solid) contours show negative (positive) zonal winds which implies a strengthening (weakening) of the prevalent trade winds. The units are ºC and m/s/ for SST and for zonal winds, respectively. (Bottom row) Vertical section of the difference in ocean temperature between future scenario and historical simulations for (c) CMIP5 and (d) CMIP6 multi-model ensemble means for June-July-August average. The blue solid (dashed) line represents the depth of the 20ºC isotherm, for the climatological mean of the historical (future scenario) period. The temperature has been latitudinally averaged from 3ºS to 3ºN. The periods taken for the historical and the scenario simulations are 1950-99 and 2050-99, respectively.

Impact of model biases

Coupled general circulation models show large biases in the tropical Atlantic region[30-33,40,41], and in particular, a warm SST bias in JJA in the eastern equatorial Atlantic, where projected changes in SST variability are largest. We explore to what extent our findings are affected by the model biases in the region. We find that the

models with smaller bias have a stronger reduction of the SST variability (Fig. 4a), a stronger reduction of the third component of the Bjerknes feedback (i.e. the thermocline feedback) (Fig. 4b) and a larger SST change between future scenario and historical (Fig. 4c). This is consistent with a previous study using different versions of the same climate model[42]. Therefore, biases in the models seem to suppress the reduction of the SST variability in a future warmer climate through a reduction of the weakening of the thermocline feedback. In light of these relationships, the reduction of future SST variability might indeed be larger than shown in this study if the models were unbiased and the reduction of the thermocline feedback would be better captured.

The reduction of the SST variability could also be affected by changes in the thermodynamical coupling between the ocean and the atmosphere. However, we find that in the CMIP models the thermodynamical mechanism is not relevant for explaining the change in the SST variance between the future climate and the historical climate periods (Fig. S3).

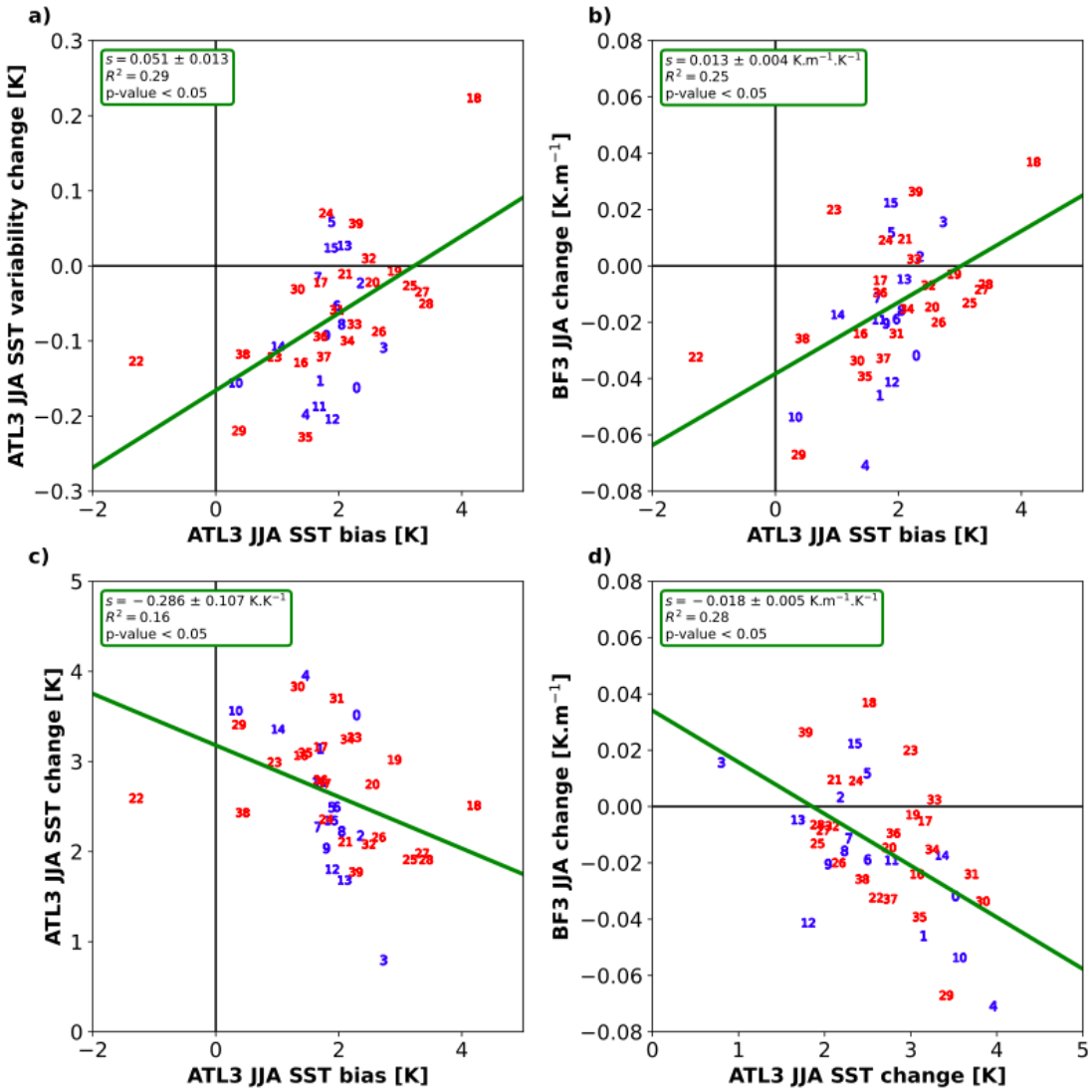

Figure 4. Impact of model biases. (a) Scatter plot of the JJA ATL3-averaged SST bias and SST variability change. The SST bias is estimated as the difference between model SST and HadI-SST over the period 1950-1999. (b) Scatter plot of JJA ATL3-averaged SST bias and BF3 change. (c) Scatter plot of JJA ATL3-averaged SST bias and mean SST change. (d) Scatter plot of JJA ATL3-averaged mean SST change and BF3 change. The change here is defined as the difference of the mean of the scenario period (2050-99) minus the mean of the historical period (1950-99).

Concluding remarks

We show that the eastern equatorial Atlantic SST variability is projected to weaken in a future warmer climate when comparing historical and future scenario simulations of the CMIP5 and CMIP6 models. The projected future weakening of the

SST variability in the CMIP models is strongly related to changes in the Bjerknes feedback. Particularly, the weakening of the third component of the Bjerknes feedback, the so-called thermocline feedback, explains up to 61% of the change in the SST variance. We find that in a warmer future climate the upper-layer of the ocean will become deeper and equatorial trade winds weaken. This together leads to a weakening of the thermocline feedback, because the thermocline decouples from the SST variability. This mechanism is remarkably different to the driving mechanisms of climate change in the equatorial Pacific, where the changes in the zonal SST gradient under greenhouse forcing are most relevant[43-45]. However, in contrast to our findings in the Atlantic, the models in the Pacific show little agreement on the sign of the change in SST gradient[45].

The future weakening of the SST could be interpreted as an amplification of the already observed weakening in the recent decades that has been attributed to a weakening of the Bjerknes feedback and a stronger thermal damping[21-23]. The role of the Bjerknes feedback in the CMIP models is key for the weakening in SST variability. However, the CMIP models do not show any significant relationship between changes in the heat fluxes and changes in the SST variability. Furthermore, the biases present in the CMIP models affect the amplitude of the SST variability. The weakening of the SST variability in the future is stronger in the models with less SST biases. Reducing the biases in the models should increase the reliability of the climate projections in the tropical Atlantic sector and greatly improve our assessment of climate change in the region.

Methods

Data. We use monthly mean model outputs obtained from the two latest CMIP international exercises: CMIP5[34] and CMIP6[35]. We use the following fields from the CMIP models: sea surface temperature (SST), zonal surface wind anomalies (UASa), surface heat fluxes and the ocean potential temperature to derive the depth of the 20ºC isotherm depth to use it as a proxy of the thermocline depth (z20 hereafter). In addition, we use the SST from the Optimum Interpolation SST analysis version 2 (OI-SST[46]) available at 1˚ by 1˚ horizontal resolution for the period 1981/12 to 2019/12; the temperature from Ocean Reanalysis System Version 4 (ORA-S4[47]) from the European Centre for Medium-range Weather forecast (ECMWF) available at

1˚ by 1˚ horizontal resolution for the period 1958/01 to 2017/12; and the zonal wind speed from ECMWF Re-Analysis (ERA)-interim[48] available at 0.5˚ by 0.5˚ horizontal resolution for the period 1979/01 to 2018/12 were used to estimate the three components of the Bjerknes feedback over the period 1982/01-2017/12. We investigate future climate changes in the equatorial Atlantic using the highest emissions future scenarios, rcp85 and ssp585, for CMIP5 and CMIP6, respectively. The climate models used in this study are listed in Table 1. All model data has been interpolated to a common horizontal 1ºx1º grid.

Statistical metrics. We use the standard deviation of the June-July-August (JJA) SST anomalies (SSTa) and the May-June-July (MJJ) zonal surface wind anomalies (UASa) as metrics to investigate the changes in variability between the simulated historical and future climate periods. The season JJA (MJJ) is chosen for the SST (UAS) variability as it is the season of largest SST (UAS) variability in CMIP5 and CMIP6 models. For this analysis we use the 50-yr periods January 1950 to December 1999 and January 2050 to December 2099 for the historical and scenario simulations, respectively. We calculate the monthly anomalies by subtracting the seasonal cycle evaluated on each time period. We remove all linear trends prior to this analysis.

Quantification of dynamical ocean-atmosphere feedbacks. We compute the three components of the Bjerknes feedback that involve SST, thermocline depth and zonal surface winds to explore the potential dynamical drivers of the future changes in the SST variability[49]. The three components of the Bjerknes feedback are estimated through linear regression of (1) western equatorial Atlantic (3ºS-3ºN, 40ºW-20º; ATL4) zonal wind stress anomalies upon eastern equatorial Atlantic (3ºS-3ºN, 20ºW-0ºN; ATL3), (2) equatorial thermocline slope anomalies regressed onto ATL4 zonal wind stress anomalies and (3) SSTa in ATL3 upon thermocline depth anomalies in ATL3. The equatorial thermocline slope is computed as the difference between the mean z20 in ATL3 and ATL4.

Acknowledgements

The CMIP6 data can be found at https://esgf-data.dkrz.de/search/cmip6-dkrz/. The CMIP5 data can be found at https://esgf-node.llnl.gov/search/cmip5/. This study was partially supported by the German Federal Ministry of Education and Research as part of the BANINO project (03F0795A). The work was supported by the H2020 TRIATLAS project (grant 817578) and the ERC STERCP project (grant 648982). We

also acknowledge Norwegian national computing and storage resources provided by UNINETT Sigma2 AS (NN9039K, NS9039K, NN9385K, NS9207k).

Author contributions:

LC, NK, SK, IR, LS and ES designed the research. LC and AP performed all the analysis and prepared the figures. LC and AP wrote the first draft. All authors read and commented on the text.

Competing interests:

No authors have any competing interests.

Watanabe, M. et al. Uncertainty in the ENSO amplitude change from the past to the future. Geophys. Res. Lett. 39, L20703 (2012).

References

1. McPhaden, M. J., Zebiak, S. E. & Glantz, M. H. ENSO as an integrating concept in Earth science. *Science* **314,** 1740–1745 (2006).

2. Timmermann, A. et al. El Niño–Southern Oscillation complexity. *Nature*, **559**(7715), 535–545 (2018).

3. Keenlyside, N. & Latif, M. Understanding equatorial Atlantic interannual variability. *J Climate* **20**(1):131–142. https ://doi.org/10.1175/jcli3 992.1 (2007).

4. Lübbecke, J et al. Equatorial Atlantic variability—modes, mechanisms, and global teleconnections. *Wiley Interdiscip Rev Climate Change* **9**(4):1–18. https://doi.org/10.1002/wcc.527 (2018).

5. Zebiak S. Air–sea interaction in the Equatorial Atlantic Region. *J Climate* **6**(8):1567–1586. https ://doi.org/10.1175/1520-0442(1993)006%3c156 7:aiite a%3e2.0.co;2 (1993).

6. Lübbecke, J. et al. Equatorial Atlantic variability—Modes, mechanisms, and global teleconnections. *WIREs Clim Change* 9:e527. https://doi.org/10.1002/wcc.527 (2018).

7. Hirst, A. & Hastenrath, S. Atmosphere-ocean mechanisms of climate anomalies in the Angola-Tropical Atlantic sector. *J Phys Oceanogr* **13**(7):1146–1157. https ://doi.org/10.1175/1520-0485(1983)013%3c114 6:aomoc a%3e2.0.co;2 (1983).

8. Nobre, P. & Shukla, J. Variations of SST, wind stress and rainfall over the tropical Atlantic and South America. *J Climate* **9**(May):2464–2479. https://doi.org/10.1175/1520-0442(1996)009%3c246 4 (1996).

9. Gu, G, & Adler, R. Seasonal evolution and variability associated with the West African monsoon system. *J Clim* **17**(17):3364–3377 (2004).

10. Boyd, A., Tauntonclark, J. & Oberholster, G. Spatial features of the near-surface and midwater circulation patterns off western and southern South Africa and their role in the life histories of various commercially fished species. *S. Afr. J. Mar. Sci.* **12**, 189206 (1992).

11. Chenillat, F. et al. How do climate modes shape the chlorophyll-a interannual variability in the tropical Atlantic? *Geophysical Research Letters*, **48**, e2021GL093769. https://doi.org/10.1029/2021GL093769 (2021).

12. Rodríguez-Fonseca, B. et al. Are Atlantic Niños enhancing Pacific ENSO events in recent decades? *Geophys Res Lett* 36:L20705. doi:10.1029/2009GL040048 (2009).

13. Ding, H., Keenlyside, N. & Latif, M. Impact of the Equatorial Atlantic on the El Niño Southern oscillation. *Clim. Dynam.* 38, 1965–1972 (2012).

14. Polo, I., Martin-Rey, M., Rodriguez-Fonseca, B., F. Kucharski & Mechoso, C. Processes in the Pacific La Niña onset triggered by the Atlantic Niño. *Clim. Dyn.* **44**, 115–131, https://doi.org/10.1007/s00382-014-2354-7 (2015).

15. Martín-Rey, M., Rodríguez-Fonseca, B. & Polo, I. Atlantic opportunities for ENSO prediction. *Geophys. Res. Lett.* **42**, 6802–6810 (2015).

16. Exarchou, E., Ortega, P., Rodríguez-Fonseca, B. *et al.* Impact of equatorial Atlantic variability on ENSO predictive skill. *Nat Commun* 12, 1612 (2021). https://doi.org/10.1038/s41467-021-21857-2

17. García-Serrano, J., Losada, T., Rodríguez-Fonseca, B., & Polo, I. (2008). Tropical Atlantic variability modes (1979–2002). Part II: Time-evolving atmospheric circulation related to SST-forced tropical convection. *Journal of Climate*, 21(24), 6476–6497.

18. Haarsma, R. J., & Hazeleger, W. (2007). Extratropical atmospheric response to equatorial Atlantic cold tongue anomalies. *Journal of Climate*, 20, 2076–2091. https://doi.org/10.1175/JCLI4130.1

19. Losada, T., Rodríguez-Fonseca, B., & Kucharski, F. (2012). Tropical influence on the summer Mediterranean climate. *Atmospheric Science Letters*, 13(1), 36–42.

20. Mohino, E., & Losada, T. (2015). Impacts of the Atlantic equatorial mode in a warmer climate. *Climate Dynamics*, 45(7–8), 2255–2271.

21. Tokinaga H, Xie SP (2011) Weakening of the equatorial Atlantic cold tongue over the past six decades. Nat Geosci 4(4):222–226. https://doi.org/10.1038/ngeo1078

22. Prigent, A., Lübbecke, J., Bayr, T., Latif, M., & Wengel, C. (2020). Weakened SST variability in the tropical Atlantic Ocean since 2000. Climate Dynamics, 54(5–6), 2731–2744. https://doi.org/10.1007/s00382-020-05138-0

23. Silva, P., Wainer, I. & Khodri, M. Changes in the equatorial mode of the Tropical Atlantic in terms of the Bjerknes Feedback Index. Clim Dyn (2021). https://doi.org/10.1007/s00382-021-05627-w

24. Lübbecke, J. & McPhaden, M. J. Assessing the twenty first century shift in ENSO variability in terms of the Bjerknes stability index. *J. Clim.* **27,** 2577–2587 (2014).

25. Collins, M. et al. The impact of global warming on the tropical Pacific Ocean and El Niño. Nature Geosci. 3, 391–397 (2010).

26. DiNezio, P. N. et al. Mean climate controls on the simulated response of ENSO to increasing greenhouse gases. J. Clim. 25, 7399–7420 (2012).

27. Kim, T. et al. Response of El Niño sea surface temperature variability to greenhouse warming. Nature Clim. Change 4, 786–790 (2014).

28. Cai, W. et al. Increasing frequency of extreme El Niño events due to greenhouse warming. Nature Clim. Change 4, 111–116 (2014).

29. Cai, W. et al. More frequent extreme La Niña events under greenhouse warming. Nature Clim. Change 5, 132–137 (2015).

30. Li, G. & Xie, S. P. Origins of tropical-wide SST biases in CMIP multi-model ensembles. *Geophys. Res. Lett.* 39, L22703 (2012).

31. Richter, I., Xie, S. P., Behera, S. K., Doi, T. & Masumoto, Y. Equatorial Atlantic variability and its relation to mean state biases in CMIP5. *Clim. Dyn.* 42, 171–188 (2014)

32. Richter, I., Xie, S. P., Wittenberg, A. T. & Masumoto, Y. Tropical Atlantic biases and their relation to surface wind stress and terrestrial precipitation. *Clim. Dyn.* 38, 985–1001 (2012).

33. Richter, I., Tokinaga, H. An overview of the performance of CMIP6 models in the tropical Atlantic: mean state, variability, and remote impacts. *Clim Dyn* **55,** 2579–2601 (2020). https://doi.org/10.1007/s00382-020-05409-w

34. Taylor KE, Stouffer RJ, Meehl GA (2012) An overview of Cmip5 and the experiment design. Bull Am Meteorol Soc 93:485–498 doi:10.1175/BAMS-D-11-00094.1

35. Eyring, V., et al. (2015). Overview of the Coupled Model Intercomparison Project Phase 6 (CMIP6) experimental design and organisation. Geoscientific Model Development, 8(12), 10, 539–10,583 https://doi.org/10.5194/gmdd-8-10539-2015

36. Maloney, E. D., and S.-P. Xie (2013), Sensitivity of tropical intraseasonal variability to the pattern of climate warming,J. Adv. Model. Earth Syst., 5, 32–47, doi:10.1029/2012MS000171.

37. Deppenmeier, AL., Haarsma, R.J. & Hazeleger, W. The Bjerknes feedback in the tropical Atlantic in CMIP5 models. *Clim Dyn* 47, 2691–2707 (2016). https://doi.org/10.1007/s00382-016-2992-z

38. Ding, H., Keenlyside, N., Latif, M., Park, W., and Wahl, S. (2015), The impact of mean state errors on equatorial Atlantic interannual variability in a climate model, J. Geophys. Res. Oceans, 120, 1133– 1151, doi:10.1002/2014JC010384.

39. Chang, P., Zhang, R., Hazeleger, W. et al. Oceanic link between abrupt changes in the North Atlantic Ocean and the African monsoon. Nature Geosci 1, 444–448 (2008). https://doi.org/10.1038/ngeo218

40. Exarchou, E., Prodhomme, C., Brodeau, L. *et al.* Origin of the warm eastern tropical Atlantic SST bias in a climate model. *Clim Dyn* 51, 1819–1840 (2018). https://doi.org/10.1007/s00382-017-3984-3

41. Voldoire, A. et al. 2019, Role of wind stress in driving SST biases in the Tropical Atlantic, *Clim. Dyn.*, DOI:10.1007/s00382-019-04717-0, 53(5), 3481-3504.

42. Park, W., Latif, M. Resolution dependence of CO2-induced Tropical Atlantic sector climate changes. *npj Clim Atmos Sci* 3, 36 (2020). https://doi.org/10.1038/s41612-020-00139-6

43. Collins, M. et al. The impact of global warming on the tropical Pacific Ocean and El Niño. *Nat. Geosci.* 3, 391–397 (2010).

44. Heede, U. K., Fedorov, A. V. & Burls, N. J. Timescales and mechanisms for the tropical Pacific response to global warming: a tug of war between the Ocean Thermostat and weaker Walker. *J. Clim.* 33, 6101–6118 (2020).

45. Heede, U. K., Fedorov, A. V. & Burls, N. J. A stronger versus weaker Walker: understanding model differences in fast and slow tropical Pacific responses to global warming. *Clim. Dyn*. https://doi.org/10.1007/s00382-021-05818-5 (2021).

46. Reynolds RW et al. (2007) Daily high-resolution-blended analyses for sea surface temperature. J Clim 20(22):5473–5496

47. Balmaseda, M.A., Mogensen, K. and Weaver, A.T. (2013) Evaluation of the ECMWF ocean reanalysis system ORAS4. *Quarterly Journal of the Royal Meteorological Society*, 139, 1132–1161.

48. Dee, D. P., et al. 2011: The ERA-Interim reanalysis: configuration and performance of the data assimilation system. *Quart. J. Roy. Meteor. Soc.*, **137**, 553-597.

49. Lübbecke, J. F., and McPhaden, M. J. (2017), Symmetry of the Atlantic Niño mode, Geophys. Res. Lett., 44, 965– 973, doi:10.1002/2016GL071829.

Supplementary material

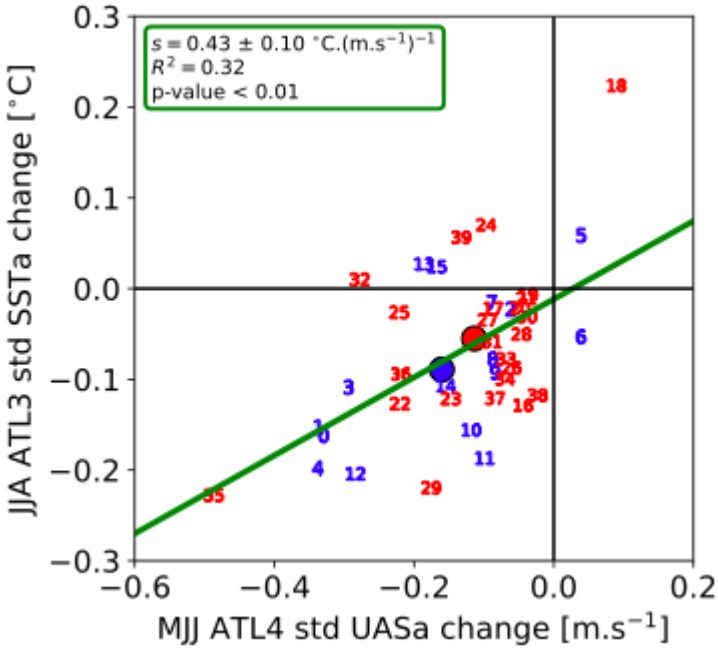

Figure S1. Linear regression between the change of the ATL3-averaged JJA SST variability and the change in ATL4-averaged MJJ uas variability. The change is defined as the difference of the mean of the scenario period (2050-99) minus the mean of the historical period (1950-99). CMIP6 (CMIP5) models are presented with blue (red) numbers and the ensemble mean with a circle of the corresponding colour.

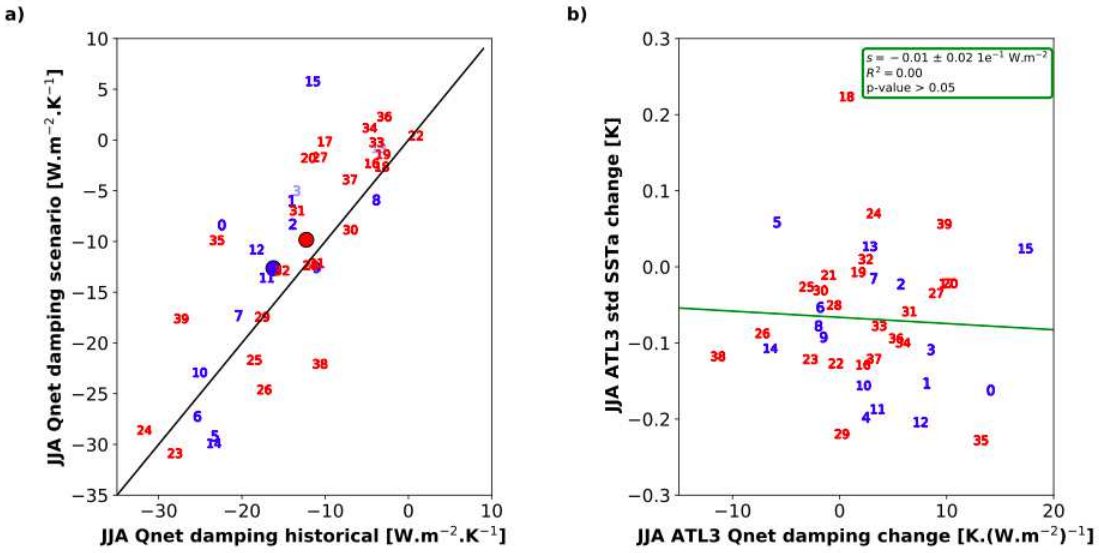

Figure S2. (a) Scatter plot of the ATL3 averaged JJA thermal damping for the historical period (1950-99) in the x axis against the ATL3 averaged JJA thermal damping for the

scenario period (2050-99) in the y axis. Transparent numbers denote the models which exhibit a non significant linear regression for either the historical or future period. The blue and dots represent the ensemble mean of the CMP6 and CMIP5 ensembles, respectively. The black line represents the no-change line and is added for easier interpretation.